

PACS numbers: 42.55.Wd; 42.60.Fc; 61.48.De
DOI: 10.1070/QE2015v045n09ABEH015804

Pulsed ytterbium-doped fibre laser with a combined modulator based on single-wall carbon nanotubes

D.V. Khudyakov, A.A. Borodkin, A.S. Lobach, S.K. Vartapetov

Abstract. **This paper describes an all-normal-dispersion pulsed ytterbium-doped fibre ring laser mode-locked by a nonlinear combined modulator based on single-wall carbon nanotubes. We have demonstrated 1.7-ps pulse generation at 1.04 μm with a repetition rate of 35.6 MHz. At the laser output, the pulses were compressed to 180 fs. We have examined an intracavity nonlinear modulator which utilises nonlinear polarisation ellipse rotation in conjunction with a saturable absorber in the form of a polymer-matrix composite film containing single-wall carbon nanotubes.**

Keywords: *fibre laser, ultrashort pulses, ytterbium, saturable absorber, single-wall carbon nanotubes.*

1. Introduction

Ultrashort pulse (USP) fibre lasers are currently widely used in many areas of science and technology where compact, reliable and sufficiently cheap light sources requiring no regular maintenance are needed. The concepts related to USP fibre laser systems have changed significantly over the past few decades: from soliton lasers with a dispersion-controlled cavity configuration and a pulse energy of several tens of picojoules to all-normal-dispersion cavity designs, which ensure pulse energies of up to several tens of nanojoules even in the case of relatively simple configurations [1]. In mode-locked ultralong fibre cavities, pulse energies of several microjoules were obtained [2]. To ensure and stabilise pulsed mode, all these schemes take advantage of an intracavity nonlinear intensity modulator. One example of such a modulator is a saturable absorber utilising photoinduced transitions in organic compounds or semiconductor heterostructures (SESAM) [3]. Such a modulator can also use nonlinear polarisation ellipse rotation (NPR) during light propagation in a nonlinear medium in combination with a polariser [4–6]. Since nonlinear pulse polarisation rotation takes place in an optical fibre of considerable length, an NPR modulator is unstable and its operation depends on external conditions. In recent years, composites containing single-wall carbon nanotubes (SWCNTs) have been intensely studied as materials for nonlinear optical modulators. The short recovery time (under 1 ps) and absorption in the range 1–1.7 μm allow SWCNTs to be used as saturable absorbers for mode locking in pulsed solid-state and fibre lasers [7–15]. Both liquid and solid media can be used as matrices for SWCNTs. SWCNT-based devices can readily be produced in the form of thin films or polymer blocks, which makes them more attractive for practical use than nonlinear semiconductor mirrors. A thin-film saturable absorber made of a carboxymethylcellulose-based polymer-matrix composite material containing single-wall carbon nanotubes (CMC–SWCNT composite) was successfully used in pulsed fibre lasers operating at 1.55 μm [16]. The main advantages of SWCNT-containing polymer films over SESAMs are that such films are relatively easy to produce and that they can be used in ring laser configurations, where a saturable absorber operating in transmission mode is needed.

On the other hand, in contrast to NPR mode locking, mode locking in a laser with a saturable absorber is more stable and self-starting. Polymer–SWCNT composite materials are used primarily for USP generation in erbium-doped fibre lasers. One reason for this is that their output wavelength (1.55 μm) lies at the maximum in the absorption spectrum of SWCNTs. Another reason is that there are standard (not microstructured) single-mode fibres that have anomalous group velocity dispersion at this wavelength. In anomalous-dispersion fibre cavities, pulses usually propagate in the soliton regime when there is a balance between the effects of dispersion and nonlinearity in a transparent medium. The output power of such soliton lasers is not very high, and thin-film SWCNT-containing modulators can be used under such conditions with no thermal destruction hazard.

A different situation occurs in the case of ytterbium-doped fibre lasers, which emit at a wavelength near 1 μm and the soliton regime of USP generation is thus difficult to ensure because there are no standard single-mode fibres with anomalous dispersion around $\lambda \sim 1$ μm. For this reason, an all-normal-dispersion cavity configuration is preferable in the case of USP ytterbium-doped fibre lasers. Pulse generation in the dissipative soliton regime is then also possible, provided that self-phase modulation and dispersion-induced pulse broadening are compensated by a wavelength-selective element [17–20]. Such oscillators usually have high output pulse energy, which may reach several microjoules. Because of this, the use of SWCNT-containing polymer films as intracavity modulators presents problems related to their optical damage resistance and long-term operation modes.

In this report, we propose a combined intracavity modulator configuration for the mode locking of pulsed fibre lasers

D.V. Khudyakov, A.A. Borodkin, S.K. Vartapetov Physics Instrumentation Center, A.M. Prokhorov General Physics Institute, Russian Academy of Sciences, Troitsk, 142190 Moscow, Russia; e-mail: khudyakov@pic.troitsk.ru, borodkin_andrey@mail.ru, svart@pic.troitsk.ru;
A.S. Lobach Institute of Problems of Chemical Physics, Russian Academy of Sciences, prosp. Akad. Semenova 1, 142432 Chernogolovka, Moscow region, Russia; e-mail: lobach@icp.ac.ru

Received 11 March 2015; revision received 21 May 2015
Kvantovaya Elektronika **45** (9) 813–818 (2015)
Translated by O.M. Tsarev

using a CMC–SWCNT thin-film saturable absorber in combination with NPR. On the one hand, this combined mode locking ensures self-starting USP generation. On the other, it ensures that the peak intensity incident on the CMC–SWCNT film is below its damage threshold. It is worth noting that USP fibre laser configurations with SWCNT-based intracavity modulators and mode locking partially supported by NPR were demonstrated previously [21–24]. Here we examine (for the first time to our knowledge) the mechanism of the interplay between the saturable absorber and nonlinear polarisation rotation for intracavity pulse energy stabilisation well below the damage threshold of the thin-film saturable absorber.

2. Pulsed fibre laser

As components of the polymer-matrix composite material for the fabrication of thin-film modulators, we used carboxymethylcellulose (medium viscosity carboxymethylcellulose sodium salt, Sigma) and SWCNTs (Carbon Nanotechnologies, Inc.) with a nanotube diameter of 1.05 ± 0.15 nm. A thin CMC–SWCNT film was produced as described by Tausenev et al. [16], by casting an SWCNT suspension in an aqueous CMC solution onto a smooth surface, followed by water evaporation at a constant temperature of 40 °C for 24 h.

In our experiments, we used a 10-μm-thick film with a small-signal transmission of 88% at 1.04 μm. Figure 1 shows a schematic of the pulsed ytterbium-doped fibre ring laser. The passive fibre segments were made of single-mode fibre with core and cladding diameters of 6 and 125 μm. The active segment, 2 m in length, was made of GTWave fibre, consisting of an active fibre and pump fibre in contact, encased together in an outer polymer cladding. The cladding diameters of the active and pump fibres were 125 and 100 μm, respectively, and the core diameter of the active fibre was 6 μm. The output of a multimode laser diode with a maximum average power of 9 W at $\lambda_p = 976$ nm was coupled into the pump fibre. To the total length of the fibre section of the cavity (4.6 m) corresponded a total group velocity dispersion of 0.13 ps^2. The light was outcoupled from and again coupled into the fibre using collimators (*3*). The polarisation state was controlled using a quarter-wave plate (WP1), half-wave plate (WP2) and Glan–Thompson polariser. The free-space part of the oscillator included a thin-film spectral filter with a transmission bandwidth (full width at half maximum) of 10 nm. The filter allowed the centre wavelength of the laser to be tuned in the range 1.03–1.05 μm.

The CMC–SWCNT polymer-matrix film was placed on a single-axis translation stage, which allowed us to move the film along the optical axis between two lenses (f = 3.5 cm) forming a telescope system. Shifting the film changed the spot diameter of the incident beam and, accordingly, the incident intensity. The CMC–SWCNT film was sandwiched between two 150-μm-thick glass plates in immersion oil to prevent contact with air or water. Moreover, this configuration improved the optical quality and uniformity of the sample, raising the optical damage resistance of the thin-film modulator. Unidirectional lasing in the ring cavity was ensured by a fibre isolator. In the absence of the CMC–SWCNT film in the cavity, pulsed operation was ensured by NPR at an absorbed pump power of 500 mW. Pulse trains had a small harmonic modulation with a frequency of 1.4 MHz (Fig. 2a). The pulse repetition rate was 35.6 MHz. In this regime, there was no self-starting of pulsed operation after the lasing had been interrupted for a short time. USP generation was only resumed after the optical axes of the wave plates were slightly tilted or the pump power was raised.

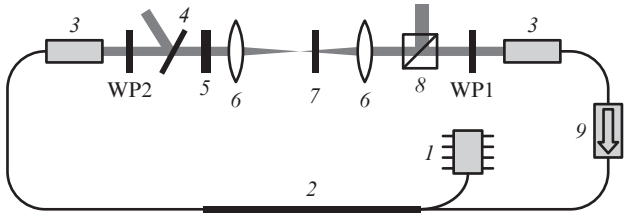

Figure 1. Schematic of the ytterbium-doped fibre ring laser: (*1*) pump laser diode ($\lambda_p = 976$ nm); (*2*) active ytterbium-doped fibre; (*3*) collimator; (*4*) glass plate; (*5*) spectral filter; (*6*) lens; (*7*) CMC–SWCNT composite film; (*8*) polariser; (*9*) isolator; (WP1, WP2) quarter- and half-wave plates.

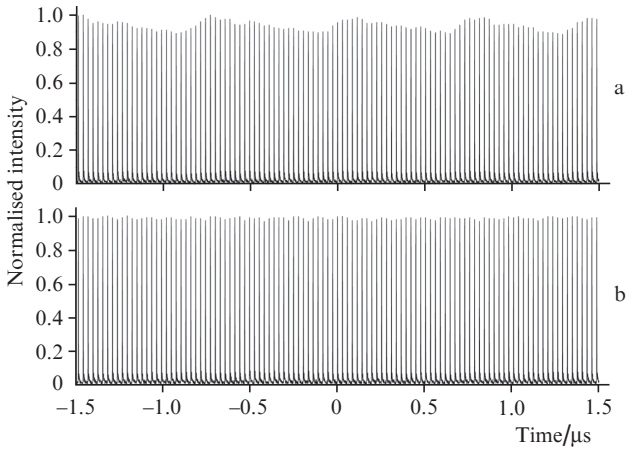

Figure 2. Oscilloscope traces of the pulsed fibre laser output (a) with no modulator and (b) with a CMC–SWCNT modulator in the cavity.

When the CMC–SWCNT film was placed in the cavity near the waist of the telescope system, there was no modulation of pulse trains (Fig. 2b) and self-starting pulsed operation was observed. Figure 3 presents an oscilloscope trace illustrating the self-starting of pulsed lasing after short-term laser beam interruption in the cavity. It is seen that the mode-locking build-up time after the cavity is opened is as short as ~300 μs and that a stable USP generation level is reached just after the first spike, with no long-term transient oscillations. In this regime, pulse generation is least dependent on fibre bends and ambient temperature. The polariser placed in the cavity was also used to outcouple the laser radiation, whose average power was 24 mW, which corresponded to a pulse energy of 0.7 nJ.

Output emission spectra in pulsed operation mode after reflection from the glass plate (*4*) and at the polariser output (Fig. 4) were measured on a Yokogawa AQ6370C spectrometer. As seen in Fig. 4, the spectra have sharp edges, suggesting that the laser operated in the normal dispersion regime. The centre wavelength and full width at half maximum of the spectrum were 1043 and 19 nm, respectively. The pulse autocorrelation function was measured at the polariser output using noncollinear second harmonic generation in a nonlinear crystal. Under the assumption that the pulses had a Gaussian shape, their full width at half maximum was determined to be

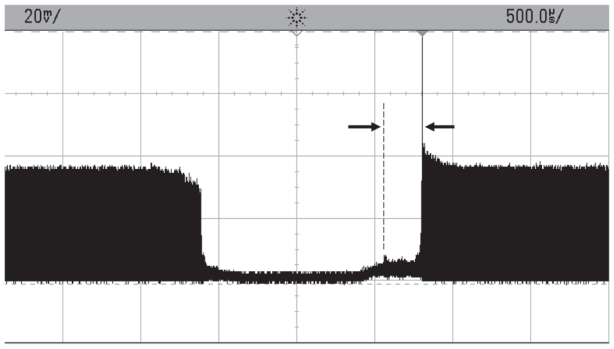

Figure 3. Oscilloscope trace of the pulsed fibre laser output illustrating the self-starting of pulsed operation after short-term beam interruption in the cavity. The arrows mark the time interval between the instant when the cavity was opened and pulsed operation onset. The dashed line indicates the instant when the cavity was opened. There is a sharp spike at the end of the pulse initiation process.

1.7 ps. At the oscillator output, the pulses were compressed by a grating pair with a ruling density of 600 lines mm^{-1}. The grating separation for optimal compression was 68 mm, which corresponded to an anomalous dispersion of -0.11 ps^2. The compressed pulse duration, determined from the autocorrelation trace of the pulses, was 183 fs, which corresponded to a compression factor of ~9. The pulse autocorrelation traces before and after compression are presented in Fig. 5. The compressed pulses have essentially no pedestal, which points to chirp linearity and suggests that higher order dispersion and nonlinear self-phase modulation make an insignificant contribution when a pulse propagates through the fibre laser cavity.

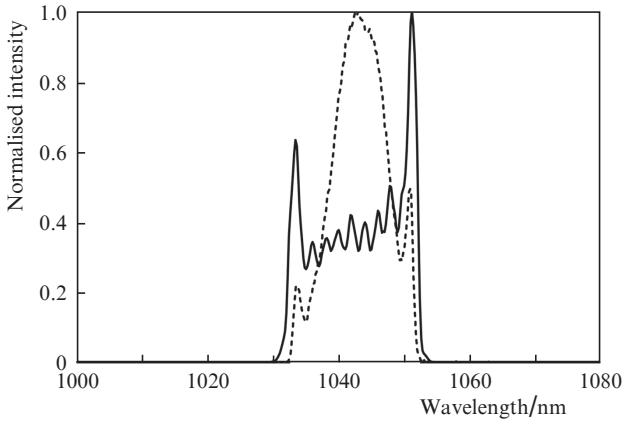

Figure 4. Emission spectra of the fibre laser in pulsed operation mode after reflection from the glass plate (solid line) and at the polariser output (dashed line).

Previously, we studied the nonlinear optical properties of CMC–SWCNT composite films using a longitudinal scanning method [25]. The absorption saturation intensity and optical damage threshold of the composite films were determined to be I_{sa} = 52 MW cm^{-2} and I_d = 800 MW cm^{-2}. As shown earlier [26], for stable USP generation in lasers with a fast saturable absorber it is necessary that the absorber operate at intensities about a factor of 10 above the saturation intensity. In our case, this corresponds to an intensity of 520 MW cm^{-2}, which approaches the damage threshold I_d. It is

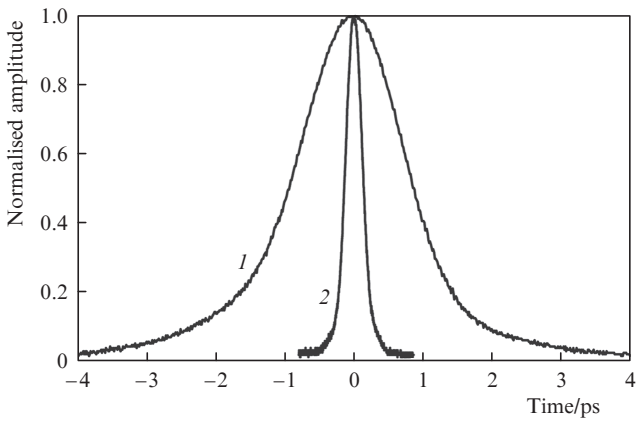

Figure 5. Autocorrelation traces of fibre laser pulses (*1*) before and (*2*) after compression.

worth noting that, in the first instance, pulse generation is initiated by several large-amplitude oscillations, whose intensity is occasionally several times the peak intensity characteristic of stable generation. For this reason, the modulator film becomes damaged at the instant of pulse initiation when the peak intensity of stable generation is a factor of 3–4 lower than the damage threshold. When the sample was placed in the centre of the waist of a telescope system with a laser spot diameter of 26 μm (incident peak intensity of 187 MW cm^{-2}), it was damaged at the instant of pulse initiation. At a beam diameter of 40 μm (incident peak intensity of 79 MW cm^{-2}), the sample remained intact and we observed stable pulse generation with fast self-starting. With increasing beam diameter, the time needed for self-starting increased. No self-starting occurred at a beam diameter of 152 μm (peak intensity of 5.5 MW cm^{-2}). Thus, the combined modulator under consideration ensures stable USP generation at peak intensities incident on the absorber film that are below the optical damage threshold by more than one order of magnitude. The observed effect is due to NPR and shows up as a reduction in transmission with increasing peak intensity, which is analysed in greater detail in the next section.

3. Discussion

When an elliptically polarised light pulse propagates in a nonlinear optical fibre, its polarisation ellipse experiences nonlinear rotation. Using the Jones matrix formalism and assuming that the medium is isotropic, we can write the matrix operator for NPR in the fibre in the form [27]

$$\mathrm{NPR}^{\mathrm{C}} = \begin{pmatrix} e^{i\Phi_+} & 0 \\ 0 & e^{i\Phi_-} \end{pmatrix}, \quad (1)$$

where $\Phi_\pm = 2/3\gamma L(|A_\pm|^2 + 2|A_\mp|^2)$ is the nonlinear phase shift; L is the fibre length; $\gamma = 2\pi n_2/(\lambda A_{\mathrm{eff}})$ is the nonlinearity coefficient; n_2 is the nonlinear refractive index; A_{eff} is the effective beam area; and λ is the wavelength of the light. It is convenient to represent the field amplitude in a linear (L) and a circular (C) basis. The transition from one basis to the other can be represented by the unitary transformation matrices

$$A^{\mathrm{L}} = \begin{pmatrix} A_x \\ A_y \end{pmatrix}, \; A^{\mathrm{C}} = \begin{pmatrix} A_+ \\ A_- \end{pmatrix}, \; A^{\mathrm{C}} = U\begin{pmatrix} A_x \\ A_y \end{pmatrix}, \; A^{\mathrm{L}} = U^+\begin{pmatrix} A_+ \\ A_- \end{pmatrix},$$

where

$$U = \frac{1}{\sqrt{2}}\begin{pmatrix} 1 & \mathrm{i} \\ 1 & -\mathrm{i} \end{pmatrix}, \quad U^{+} = \frac{1}{\sqrt{2}}\begin{pmatrix} 1 & 1 \\ -\mathrm{i} & \mathrm{i} \end{pmatrix}. \tag{2}$$

In the linear basis, the transformation matrix of a wave plate has the general form

$$\mathrm{WP}(\Delta,\theta) = \begin{pmatrix} \cos^2\theta + \mathrm{e}^{-\mathrm{i}\Delta}\sin^2\theta & (1-\mathrm{e}^{-\mathrm{i}\Delta})\sin\theta\cos\theta \\ (1-\mathrm{e}^{-\mathrm{i}\Delta})\sin\theta\cos\theta & \mathrm{e}^{-\mathrm{i}\Delta}\cos^2\theta + \sin^2\theta \end{pmatrix}, \tag{3}$$

where the angles $\Delta = \pi$ and $\pi/2$ correspond to a half-wave and a quarter-wave plate, respectively, and θ is the angle between the optical axis of the wave plate and the polariser axis. The transformation matrix of a polariser whose axis is parallel to the x component of the field has the form

$$\mathrm{P} = \begin{pmatrix} 1 & 0 \\ 0 & 0 \end{pmatrix}. \tag{4}$$

A general expression for the transformation of field components can be obtained by tracing the ring cavity in the clockwise sense starting at the polariser output:

$$A_{\mathrm{out}}^{\mathrm{L}} = P\mathrm{WP}(\pi,\theta_2)U^{+}\mathrm{NPR}^{\mathrm{C}}U\mathrm{WP}\left(\frac{\pi}{2},\theta_1\right)A_{\mathrm{in}}^{\mathrm{L}}. \tag{5}$$

The transmittance due to the NPR in the fibre is

$$T_{\mathrm{NPR}} = I_{\mathrm{out}}/I_{\mathrm{in}}, \tag{6}$$

where $I = (|A_x|^2) + (|A_y|^2)$.

Figure 6 shows the transmittance of the NPR modulator at different angles θ_1 of the quarter-wave plate. The transmittance is seen to be a periodic function of the peak pulse intensity in the fibre. The change in the latter in going from a minimum to a maximum in transmittance corresponds to a rotation of the polarisation ellipse of the light pulse through 90°. The modulation depth and period depend on the ellipticity of the light launched into the fibre, which is set by the angle θ_1 of the quarter-wave plate. Varying the angle θ_2 of the half-wave plate, we can ensure a maximum or minimum in transmittance at zero intensity. It is worth noting that the curves in Fig. 6 are obtained under the assumption that the peak intensity remains constant as the pulse propagates through the fibre. Numerical simulation taking into account transmission losses in the optical components and amplification in the active part of the cavity indicated that the error of the analytical approach did not exceed 15% for the position of extrema in the transmittance of the NPR modulator as a function of the peak pulse intensity at the fibre input. This error is admissible in analysis below.

A single pulse separates out from the stochastic pulse background of free-running laser operation when the transmission of the modulator increases with peak intensity. In view of this, the angle θ_2 was adjusted so as to ensure a minimum in transmittance at zero intensity. The modulator then operated as a saturable absorber between the minimum and maximum in transmittance, with the possibility of initiating pulse generation. To avoid pulse generation instability due to Q-switching, the angle θ_1 of the quarter-wave plate was adjusted so that the NPR modulation depth did not exceed 2%, which corresponded to a nearly circular pulse polarisation.

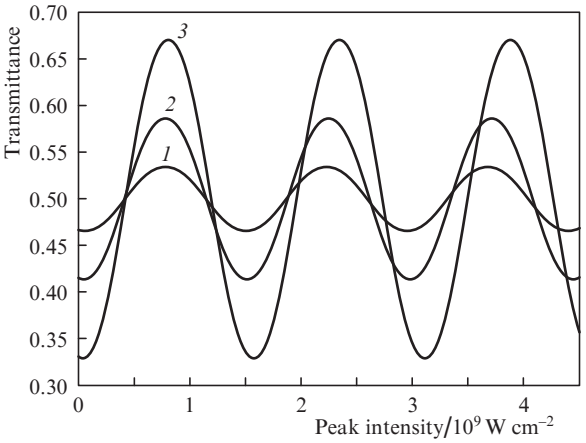

Figure 6. Transmittance as a function of the peak pulse intensity in the fibre for the NPR effect at different angles θ_1 and θ_2 of the WP1 and WP2 wave plates: $\theta_1 = (1) -43°, (2) -40°$ and $(3) -35°$; $\theta_2 = (1)\ 20°, (2)$ 22° and (3) 25°. The curves were obtained using relations (5) and (6).

Because of the saturation effect, the absorption coefficient of the CMC–SWCNT thin-film modulator as a function of incident intensity is given by

$$\alpha(I) = \frac{A_0}{1 + I/I_{\mathrm{s}}} + B, \tag{7}$$

where A_0 and B are the linear saturable and nonsaturable absorption components, respectively [28]. In the weak absorption approximation, the expression for transmittance $T_{\mathrm{nt}}(I) = \exp[-\alpha(I)L]$ can be written in the form

$$T_{\mathrm{nt}}(I) = T_{\mathrm{ns}} - \frac{\Delta T}{1 + I/I_{\mathrm{sa}}}, \tag{8}$$

where ΔT is the saturable-absorption-induced change in transmittance; T_{ns} is the nonsaturable component of transmittance; and L is the thickness of the sample. The parameters of the CMC–SWCNT film used in our experiments are $T_{\mathrm{ns}} = 0.9$, $\Delta T = 0.02$ and $I_{\mathrm{sa}} = 52$ MW cm^{-2}.

Figure 7 shows the $T_{\mathrm{nt}}(I)$ curve for the CMC–SWCNT film and indicates the region of stable pulse generation under the conditions of the combined modulator, when there was no optical damage and self-starting persisted. The transmittance of the combined modulator is

$$T = T_{\mathrm{NPR}}T_{\mathrm{nt}}. \tag{9}$$

Figure 8 shows the nonlinear transmittance as a function of peak intensity for the CMC–SWCNT film, NPR modulator and combined modulator. The curves were constructed for the wave plate angles used in our pulsed fibre laser: $\theta_1 = -44.5°$ and $\theta_2 = 18°$. The peak power for stable pulse generation is indicated by a vertical dashed line, which passes near the maximum in the transmittance curve of the combined modulator. The decrease in transmittance with increasing peak intensity to the right of the stable generation line prevents instability due to Q-switching. A similar USP generation stabilisation effect occurs in the case of two-photon absorption of incident light at high intensities in SESAMs [29]. Moreover, in the stable pulse generation regime, the peak power of the light incident on the CMC–SWCNT film

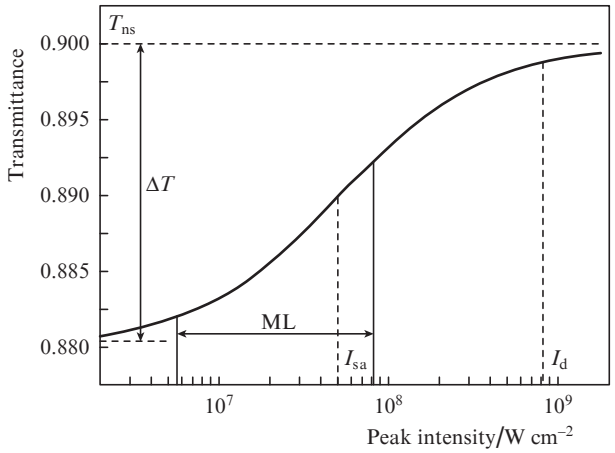

Figure 7. Transmittance of the CMC–SWCNT thin-film modulator vs. peak intensity incident on the film: (ML) region of stable self-starting pulsed operation. The high-intensity boundary of the ML region is determined by optical damage to the film at the instant of pulse initiation, and the low-intensity boundary, by the lack of self-starting pulsed operation.

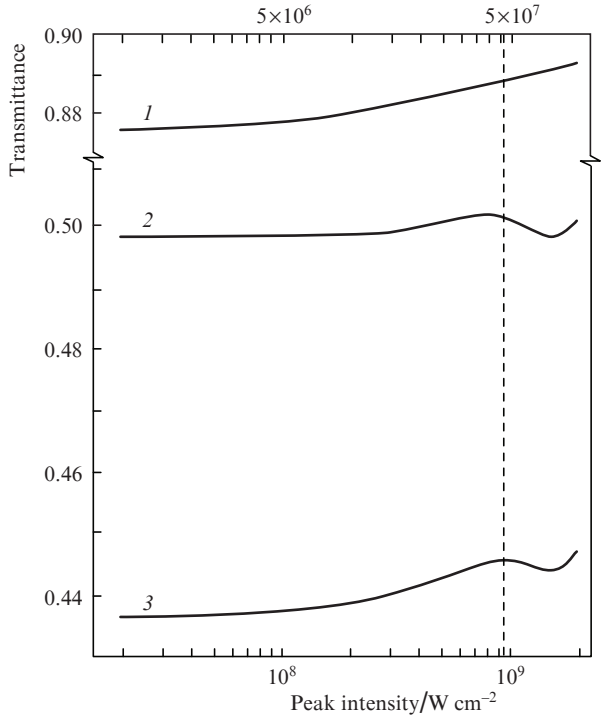

Figure 8. Transmittance as a function of peak pulse intensity in the fibre for the (*1*) CMC–SWCNT modulator, (*2*) NPR modulator and (*3*) combined modulator. The values 5×10^6 and 5×10^7 W cm^{-2} correspond to the peak intensity incident on the film of the CMC–SWCNT modulator. The curve for the NPR modulator corresponds to wave plate angles $\theta_1 = -44.5°$ and $\theta_2 = 18°$. The dashed line indicates the peak intensity for stable pulse generation.

is well below the damage threshold of the thin-film modulator, which improves its long-term reliability.

As mentioned above, the beam was outcoupled from the laser cavity using a polariser. In the laser configuration described above, the beam at the output of WP2 has nearly circular polarisation. As a result, the polariser removes almost half of the incident power. If no polariser is used for light outcoupling, and it is necessary to considerably reduce the cavity loss, a different scheme can be employed for polarisation control. Two wave plates are then used in the WP1 section: a quarter-wave and a half-wave plate, oriented at angles θ_1 and θ_2 to the polariser axis. The WP2 section contains one quarter-wave plate, mounted at an angle θ_3. If the relations $\theta_3 - \theta_1 = \pi/2$ and $\theta_2 - \theta_1 = \pi/4$ are met, the NPR modulator operates as a saturable absorber, minimising the loss in the polariser circuit. As above, the modulation depth and ellipticity of the light circulating in the cavity are determined by the angle θ_1 of the quarter-wave plate. When such an alternative is used, the light can be outcoupled from the cavity by a fibre coupler. The proposed combined mode locking method is also suitable for thin-film saturable absorbers based on polymer–graphene and polymer–MoS_2 composite materials.

4. Conclusions

A pulsed ytterbium-doped fibre laser with a pulse duration of 1.7 ps at a wavelength of 1.04 μm has been demonstrated. The fibre section of its cavity is made entirely of normal group velocity dispersion fibres. Mode locking is ensured by a SWCNT-based thin-film modulator in combination with nonlinear polarisation ellipse rotation. A model has been proposed for the operation of the combined modulator, in which the light intensity necessary for stable pulse generation is substantially lower than the damage threshold of the SWCNT-containing composite film, which opens up the possibility of using a flexible and simple process to produce SWCNT-containing films for USP generation in fibre lasers. Another distinctive feature of the combined modulator is the self-starting of USP generation, in contrast to pulse generation based only on polarisation ellipse rotation in fibre, which is not self-starting. In the early stages of pulse formation, the SWCNT-based saturable absorber helps to separate out the most intense pulse from the stochastic noise of free-running laser operation, thereby accelerating self-starting.

Acknowledgements. We are deeply grateful to M.N. Gerke for valuable discussions and support of this work.

References

1. Fermann M.E., Galvanauskas A., Sucha G., Harter D. *Appl. Phys. B*, **65**, 259 (1997).
2. Kobtsev S., Kukarin S., Fedotov Y. *Opt. Express*, **16**, 21936 (2008).
3. Okhotnikov O., Grudinin A., Pessa M. *New J. Phys.*, **6**, 177 (2004).
4. Stolen R.H., Botineau J., Ashkin A. *Opt. Lett.*, **7**, 512 (1982).
5. Kobtsev S.M., Smirnov S.V. *Laser Phys.*, **21**, 272 (2011).
6. Kobtsev S., Kukarin S., Smirnov S., Turitsyn S., Latki A. *Opt. Express*, **17**, 20707 (2009).
7. Fong K.H., Kikuchi K., Goh C.S., Set S.Y., Grange R., Haiml M., Schlatter A., Keller U. *Opt. Lett.*, **32**, 38 (2007).
8. Schmidt A., Rivier S., Steinmeyer G., Yim J.H., Cho W.B., Lee S., Rotermund F., Pujol M.C., Mateos X., Aguilo M., Diaz F., Petrov V., Griebner U. *Opt. Lett.*, **33**, 729 (2008).
9. Cho W.B., Yim J.H., Choi S.Y., Lee S., Griebner U., Petrov V., Rotermund F. *Opt. Lett.*, **33**, 2449 (2008).
10. Schibli T.R., Minoshima K., Kataura H., Itoga E., Minami N., Kazaoui S., Miyashita K. *Opt. Express*, **13**, 8025 (2005).
11. Khudyakov D.V., Lobach A.S., Nadtochenko V.A. *Appl. Opt.*, **48**, 1624 (2009).
12. Khudyakov D.V., Lobach A.S., Nadtochenko V.A. *Opt. Lett.*, **35**, 2675 (2010).

13. Yamashita S., Inoue Y., Maruyama S., Murakami Y., Yaguchi H., Jablonski M., Set S.Y. *Opt. Lett.*, **29**, 1581 (2004).
14. Rozhin A.G., Sakakibara Y., Namiki S., Tokumoto M., Kataura H., Achiba Y. *Appl. Phys. Lett.*, **88**, 051118 (2006).
15. Sakakibara Y., Rozhin A.G., Kataura H., Achiba Y., Tokumoto M. *Jpn. J. Appl. Phys.*, **44**, 1621 (2005).
16. Tausenev A.V., Obraztsova E.D., Lobach A.S., Konov V.I., Konyashchenko A.V., Kryukov P.G., Dianov E.M. *Kvantovaya Elektron.*, **37**, 847 (2007) [*Quantum Electron.*, **37**, 847 (2007)].
17. Chong A., Buckley J., Renninger W., Wise F. *Opt. Express*, **14**, 10095 (2006).
18. Chong A., Buckley J., Renninger W., Wise F. *Opt. Lett.*, **32**, 2408 (2007).
19. Kharenko D.S., Shtyrina O.V., Yarutkina I.A., Podivilov E.V., Fedoruk M.P., Babin S.A. *Laser Phys. Lett.*, **9**, 662 (2012).
20. Mortag D., Wandt D., Morgner U., Kracht D., Neumann J. *Opt. Express*, **19**, 546 (2011).
21. Liu Y., Zhao X., Liu J., Hu G., Gong Z., Zheng Z. *Opt. Express*, **22**, 21012 (2014).
22. Kobtsev S., Kukarin S., Fedotov Y. *Laser Phys.*, **21**, 283 (2011).
23. Kelleher E.J.R., Travers J.C., Sun Z., Rozhin A.G., Ferrari A.C., Popov S.V., Taylor J.R. *Appl. Phys. Lett.*, **95**, 111108-3 (2009).
24. Castellani C. E. S., Kelleher E.J.R., Travers J.C., Popa D., Hasan T., Sun Z., Flahaut E., Ferrari A.C., Popov S.V., Taylor J.R. *Opt. Lett.*, **36**, 3996 (2011).
25. Khudyakov D.V., Borodkin A.A., Lobach A.S., Ryzhkov A.V., Vartapetov S.K. *Appl. Opt.*, **52**, 150 (2013).
26. Honninger C., Paschotta R., Morier-Genoud F., Moser M., Keller U. *J. Opt. Soc. Am. B*, **16**, 46 (1999).
27. Haus H.A., Ippen E.P., Tamura K. *IEEE J. Quantum Electron.*, **30**, 200 (1994).
28. Rozhin A.G., Sakakibara Y., Kataura H., Matsuzaki S., Ishida K., Achiba Y., Tokumoto M. *Chem. Phys. Lett.*, **405**, 288 (2005).
29. Thoen E.R., Koontz E.M., Joschko M., Langlois P., Schibli T.R., Kartner F.X., Ippen E.P., Kolodziejs L.A. *Appl. Phys. Lett.*, **74**, 3927 (1999).